THE TRICKS AND TRIVIA OF LIQUID SCINTILLATOR HADRON CALORIMETRY

L. R. Sulak

Invited Talk
FNAL Calorimeter Workshop
9 May 1975

Contents

1. Introduction to the Calorimeters

This review summarizes some of the experience of our group in liquid scintillation hadron calorimetry. My task, as requested by Muzaffer Atac, is "to review what does not get into the journals". Therefore, this paper contains the tricks and the trivia as practiced in Fermilab Experiment 1A and in Brookhaven Experiment 613.

For concreteness, we will consider two operating calorimeters. The first, shown in Fig. 1a, is the FNAL neutrino experiment 1A hadron calorimeter.[1] This device is a large, rectangular box filled with pure liquid scintillator. It measures the energy of hadronic showers produced by neutrino interactions occurring in the liquid. It is eight absorption lengths[2] long (fourteen radiation lengths) and four absorption lengths wide. The device contains sixty tons of pure liquid, and is viewed by two hundred five-inch diameter photomultiplier (PM) tubes. It is optically divided into sixteen slabs, each perpendicular to the beam; each slab is viewed by twelve five-inch PM's, six on each side. The detector must measure energy deposits from 10 MeV (1/10 of a minimum ionizing particle in one slab) to 300 GeV (the maximum possible neutrino energy) i.e., it must respond over a dynamic range of 10^4. The linear sum of the signals from the twelve tubes viewing each slab goes to a pulse height analysis channel. Figure 1b shows the distribution of hadronic energy deposited in each of the sixteen slabs for a typical event. Notice that each of the first ten slabs has no energy deposition above the minimum measurable deposition (equivalent to one-tenth that deposited by a minimum ionizing particle). The vertex of an interaction

occurs in slab No. 11. The associated hadronic cascade develops and is partially absorbed before it leaves the rear of the calorimeter.

The second device that we discuss is a similar calorimeter used in Brookhaven Neutrino Experiment 613. This calorimeter, again in the shape of a rectangular box (see Fig. 2) is optically segmented into 200 cylinders, each perpendicular to the beam, eight inches square in cross section and nine feet long. The device contains thirty tons of pure liquid, and is viewed by 400 two-inch PM tubes. This detector must sense low energy hadrons ($\sim$1 GeV), typically one or two, exiting from a neutrino interaction in the liquid scintillator. The energy of the final state hadron(s) extends only to 10 GeV. However, this calorimeter must record proton recoils initiated by low energy neutrons entering the device. Detecting neutrons by their multiple interactions requires sensitivity down to 1 MeV. Again a dynamic range of 10^4 is necessary. This detector must 1) measure the energy in each cylinder, 2) measure the longitude position in the cylinder to four inches, 3) measure the time of the occurrence of an event to 0.5nsec over the three microsecond beam burst, and 4) have multiple event capability to record the multiple pulse signature of the pion $\rightarrow$ muon $\rightarrow$ electron decay sequence. We therefore need a <u>minimum</u> of 400 channels each of ADC and TDC.

The information recorded for a typical PM is outlined in the block diagram of Fig. 3. The recording chain is initiated by the beam gate, which opens the system for the entire beam spill. Each PM has 1) a discriminator, 2) coarse resolution event timing (50ns clock period) over the three microsecond spill, 3) fine resolution vernier

timing (interpolation within the clock period) to 0.5nsec; 4) a pair of ADC's (both high and low sensitivity) to measure the charge deposited. A second channel of coarse and vernier timings, armed by firing of the first, enables one to detect π or μ decay.

2. Why Liquid Scintillator?

The enormous size and large number of elements constrain the design of the above devices to be inexpensive, simple, reliable, stable and constantly monitorable. These requirements dictate the use of liquid scintillator as opposed to plastic scintillator or liquid argon calorimetry. (Liquid argon technology was unknown at the time of design.) Liquid scintillator offers several advantages relative to plastic: 1) lower light attenuation length (typically 3 meters vs. 1 meter), 2) inexpensiveness (approximately $1.00 per gallon vs. the price of gold at the old value!), 3) uniform light output (liquids mix uniformly), and 4) the flexibility of building any possible shape -- one simply bends a metal box and fills it with liquid.

Inexpensive liquid scintillator[3] consistsof ~60% USP light mineral oil ~35% 1,2,4 trimethylbenzene, and ~5% proprietary ingredients. For large volume applications, dilution of this scintillator by a factor of two with white mineral oil decreases the light output by only 30%. For experiments where pulse shape discrimination is necessary (the Brook's effect) the mixture changes somewhat. Experiments where the oil is exposed to low temperatures (40°F), low pour point (-20° to 0°F) naphthalene-based (vs. paraffin-based) mineral oil is necessary to avoid clouding of the scintillator.

3. Pure Liquid Devices vs. Sampling Devices

Two facts suggested that pure liquid scintillator would yield energy resolution superior to a fine-grained sampling device in the FNAL experiment: 1) The high concentration of hydrogen (ratio of carbon atoms to hydrogen atoms is 1/1.9) suggests that the energy of evaporation neutrons produced in hadronic showers may be recoverable; 2) binding energy losses are low due to the low Z of the carbon. Figure 4 shows a compendium of energy resolutions for several calorimeters with various sampling granularities that have been reported at this conference. In the 20 GeV hadronic energy range, appropriate to typical neutrino interaction at FNAL, pure liquid is superior to sampling devices.

In the low energy BNL experiment, the protons of interest would be absorbed by sampling plates. Further, this experiment requires an active shield against the neutrons which are in equilibrium with neutrinos. As is shown in Fig. 5, the attenuation length for 6 MeV neutrons is 10 cm. In travelling through the entire target of ~40 attenuation lengths, neutrons mark their presence through multiple interactions. Thus, a neutron-free event sample is obtained by insisting that the entire Brookhaven calorimeter be quiet, except for a lone cylinder in the center of the detector.

4. Guiding the Light Through the Scintillator

How does one guide light through liquid scintillator? For acceptable efficiency with several bounces, one needs an interface that is totally internally reflecting. Of all plastics only teflon,

with an index of refraction equal to 1.35, has an index smaller than that of the liquid scintillator, typically 1.47. Figure 6 displays the technique of using a scintillator-teflon interface to guide light out of the liquid. The critical angle of total internal reflection, below which all light is captured, is 24^{o}.

The teflon film[4] is typically 0.001" thick. The surface not in contact with the liquid is coated with evaporated aluminum and backed with an adhesive. The aluminum coating is necessary for thin layers ($\lesssim$1cm) of scintillator. It specularly reflects ultraviolet light produced by dE/dx loss, insuring that it travels a sufficient distance to be absorbed by the wavelength shifter. The adhesive allows one conveniently to paste the teflon film onto the container walls. One merely peals the teflon from its mylar backing (a packaging technique similar to double-sided Scotch tape), smoothes the teflon onto the aluminum (which has been prewetted with a detergent solution), and squeezes out the water. The remaining mositure evaporates through the teflon.

Figure 7 demonstrates the reflectivity of a teflon-coated module of the FNAL calorimeter. The response of the PM's to horizontal muons is displayed as a function of the distance of the muons from the phototube. One would expect (as in curve III) a $1/r^2$ variation in the amount of light collected by the tube if phase space dominates the light collection. Instead, the response of a single tube (curve I) and the response of all twelve tubes linearly added (curve II) show that the teflon is indeed working. For typically 10 bounces in this device, the change in amplitude

from the center of the calorimeter (60" from the phototubes) to the edge is ±15%. This correction is directly calibrated by muons (curve II). A similar module for FNAL Experiment 310, with 1/4" thick liquid layers, shows identical response[5] to that above with an average of 250 reflections!

The effects of the high reflectivity are evident in the pulse shape. The front edge of the pulse is sharp, carrying information on the timing of the light deposition. However, the charge collection time is long, typically 50nsec, due to many transits back and forth in the module. These are seen as regular bumps on the falling edge of the pulse.

5. Containing the Oil and Retaining Its Purity

Figure 8 shows a cross-section of the Brookhaven calorimeter. In spite of the large hydrostatic force on the walls (50,000 pounds), thin aluminum sheets (1 mm) from one wall (also 1 mm Al) to the other hold the calorimeter together and simultaneously provide optical isolation.

Although the container for the oil may well be gas tight, water tight, and jet-fuel tight, our experience is that it will still leak oil. Only fluorocarbon rubber[6] seems to keep the oil from finding its way out of a container.

To assess possible contamination of the scintillating properties of the oil, we have tested the long term stability of the scintillator under exposure to many common construction materials. Only teflon, fluorocarbon rubber, and epoxy paint (available in scotchlight white[7] for reflectivity) seem immune to

attack by the caustic trimethylbenzene. Epoxy paint is necessary for iron surfaces directly exposed to scintillator. The liquid invariably contains water from condensation which causes unconditioned iron to rust and discolor the water.

6. Transmitting the Light to the PM

We use the pressure of the oil itself to hold plexiglas windows against holes in the container of the BNL calorimeter. Fluorocarbon rubber serves as the gasket between the window and the container. Clear epoxy[8] cookies make the light connection between the plexiglass window and PM face. Inexpensive[9] RCA 8055 (4×10^6 tubes (5" diameter) and 655A (1×10^6 (2" diameter) are used. A simple printed circuit board contains the dynode resistor chain and the socket for the tube. One high voltage supply provides power for the 32 tubes of each module at BNL; a potentiometer at the base of each tube adjusts PM gain by regulating the voltage between the 5th and 6th dynodes.

7. Getting the Signal Out (Alone)

In the FNAL calorimeter, the typical signal from a minimum ionizing particle is 0.2 millivolts per tube. In a noisy environment, where wide-gap spark chambers (firing at 50 kV) are sandwiched between the faces of adjacent calorimeter modules, a system that is immune to spark noise pickup is mandatory. We utilize the phototube as a push-pull source (Fig. 9). The negative anode signal and the positive signal from the last two dynodes (capacitatively coupled) drive a shielded, balanced twisted pair line (twinax). Since the PM is an ideal current source, we passively add the signals from 12 PM's in a daisy chain. In the BNL application, the digitization electronics are housed at the PM, which avoids long cables and allows the entire module to be a Faraday cage for the electronics.

We have found it more economical to buy inexpensive tubes and amplify the signal with semiconductors, rather than buying more expensive tubes. Figure 10 shows a block diagram of a balanced amplifier, a BAL/UN transformer, and two parallel channels of digitization (each an ADC with a bilinear mode), a sensitive high resolution channel and an attenuated, low sensitivity channel.

8. What Kind of ADC?

With the full scale count limited in an ADC, the digitization error should match the calorimeter resolution. For a fractional energy resolution which goes as the reciprocal of the square root of the charge collected, the ideal ADC response goes as the square root of the charge. On the other hand, if the fractional resolution is constant (a good approximation for the FNAL calorimeter), the ADC response should be logarithmic. Charging the digitization capacitor with a quadratic or an exponential current source will produce these ADC responses. However, an excellent approximation can be achieved by piecewise, continuous functions; e.g., the Lecroy ADC, which has a sensitivity of 1/4 pc per channel for the first 128 channels and 1 pc for the next 128 channels, yielding a dynamic range of 5×10^2. To obtain a range of 10^4 one can stagger two such bilinear scales. In the BNL calorimeter, the last dynode drives a high sensitivity bilinear channel, and the signal derived three dynodes earlier, where the signal is ~30 times smaller, drives a second bilinear scale. Thus one samples large signals early in the dynode chain before saturation. With such a device, 9 bits give 3×10^3 counts when one would ordinarily need 50,000 counts with a linear ADC.

9. Equalizing, Monitoring, and Calibrating Tubes

To equalize the gain of phototubes that have been linearly added, we utilize green light-emitting diodes (to match the blue response of the scintillator). With CAMAC controlled relays at the base of each PM, we turn off all tubes but one. The light-emitting diode checks the operation of the one PM left connected. The response to such a light-emitting diode (LED) is shown in Fig. 11, where the amplitude of the LED signal has been adjusted to give the same output as a minimum ionizing particle. The signal fluctuations, which are due to photoelectron statistics, imply that a 50 keV energy deposition in the FNAL calorimeter yields one collected photoelectron. In the BNL calorimeter, where 200 cylinders make LED monitoring difficult, optical fibers transport light to each phototube.

To monitor the long-term response of the liquid and to calibrate the energy scale, we use vertical cosmic ray muons (which have a high rate -- typically 1 KC -- for these large devices). A gate is opened between each burst of the accelerator, thereby obtaining a continual cosmic-ray calibration of the entire system. To measure pile-up, etc., that might occur during the beam burst, the system is triggered by horizontal beam muons during part of the accelerator burst.

10. Verifying the Linearity of the ADC Chain

To regularly check the entire ADC chain, we inject pulses, whose amplitude spans the full 10^4 dynamic range early, in the ADC chain. A mercury pulser feeds pulses through a CAMAC controlled attenuator into the end of the twisted pair daisy chain of the FNAL system. The relay at the PM tube (see Fig. 12) switches the PM out of

and the test source into the chain (see Fig. 12). Figure 13 shows a typical check of the linearity of the system.

11. Hadronic Energy Resolution

The FNAL calorimeter has been calibrated using an incident negative hadron beam (primarily π^-'s) with energies from 15 to 150 GeV. The results are shown in Fig. 14. The fractional resolution is $\lesssim$12% for this range of hadron energies. The resolution is compared with that obtained by sampling devices and by calculations in Fig. 4. There the upper limit on hadron energy resolution in the 300 MeV region is obtained from the mass resolution for Λ production in neutrino interactions. This resolution (30%) is compatible with calculations of Gabriel[10] for this region.

12. Containment Corrections

For showers initiated late in the calorimeter, like those shown in Fig. 1b, the transition curve is truncated, and one would like to correct for partial shower containment. From the hadron calibration run, we have measured "average" shower transition curves for various incident energies (Fig. 15). These curves are fit by a simple algorithm[1]. By artificially truncating a fully-contained shower, we can fit the initial portion of the transition curve, and estimate the total energy in a shower, as if it were fully contained. We compare the results of this procedure with the actual deposition. Typically, correcting a shower that is 70% contained inflates the energy resolution by a factor of only 30%, i.e., from an energy resolution of 11% for a fully-contained shower to 14% for the truncated shower.

13. Fitting Fluctuations in the Hadronic Transition Curves

The resolution of hadron calorimetry is limited by the fluctuations between the amount of energy that goes into the hadronic component ($\pi^{\pm}$,p,n,...) vs. that which appears as electromagnetic energy (π^{o}). Figure 15 shows a measurement[10] of the energy deposited in a sampling calorimeter by pions and electrons of the same energy. Note that π^-'s produce 30% less light than e^-'s of the same energy, and that the spread is 20% vs. 8%, respectively. Nevertheless, the maximum energy deposited by the π^-'s can reach all the way up to the maximum of energy deposited by the electrons, i.e., when 100% of the π^- energy finds its way into the electronic channel via elastic charge exchange. On the other hand, the lo end of the π^- curve corresponds to a maximal loss of energy in hadronic channels to binding energy, etc.

This partition of energy is immediately seen in individual transition curves, an idealization of which is sketched in Fig. 17. Local bumps $\gtrsim$30% larger than the average transition curve are apparent. (In producing the "average" curves of Fig. 15, the local variations are averaged out.) For incident pions of fixed energy, one can fit the transition curves to minimize the RMS deviation from the mean energy of all events. Such a fit chooses to deflate the contribution of local bumps and to inflate the value of local depressions. For 25 GeV pions incident on the FNAL calorimeter, the fit decreases the RMS deviation from 14% to 11%. A contribution to this meeting[10] shows that such a decrease is primarily accomplished by removing long tails in the resolution curve, yielding a pure Gaussian resolution function.

In addition to fitting transition curves, one can use the very different characteristics of electromagnetic and hadronic showers to sample the amount of energy deposited by each in a shower. Figure 18 shows a side view of the hybrid calorimeter under construction for FNAL neutrino Experiment 310.[5,12] Here one alternates sections of low Z, high nuclear attentuation length with sections of high electromagnetic attentuation length and low collision length. Thereby one samples hadronic and electromagnetic energy depositions in the device. Typically, a low Z segment is similar to one of the 16 slabs in FNAL Experiment 1A, whereas a high Z section is a slab filled with 1/4" thick, teflon-coated lead sheets.

14. Position Determination

In the BNL calorimeter, it is necessary to determine where an individual particle traversed a cylinder along its 6' length. Figure 19 shows a conceptual side view of a cylinder with a PM at each end. The traversal position is determined in two alternate ways: 1) time of flight difference between the phototubes, and 2) normalized pulse height difference. The second scheme measures the position of via the ratio R, $R = V1 - V2/V1 + V2$, where V1 and V2 are the signals measured for left and right PM's, respectively. The position resolution obtained with this technique has been determined for muons travelling through 8 cylinders. A straight line fit to the ratios R yields the deviation shown in Fig. 20. The resolution for both this and the independent technique of time of flight is $\sigma = 4"$, factor of two times smallter than the hodoscopic grid size (8") in the other two dimensions.

Acknowledgements

Most of the tricks described in this review emanated from that idea machine, Carlo Rubbia. J. Blandino and J. McElaney were responsible for the mechanical construction, and Hans Weedon implemented the electronics. The entire staff of the High Energy Physics Laboratory, Harvard University, have devoted one-third of their time for the past four years to the realization of these detectors. W. T. Ford derived the algorithm for shower containment. The following people have also contributed to this work: A. Benvenuti, D. Cheng, D. Cline, D. DiBitonto, R. Imlay, W. Kozanecki, T. Y. Ling, A. K. Mann, F. Messing, R. L. Piccioni, J. Pilcher, D. D. Reeder, J. Rich, R. Stefanski and J. Strait.

Footnotes

1. This device is described by A. Benvenuti et al., Nuc. Inst. and Math., Vol. 125 #2, p. 447 (Ap. 15, 1975).

2. We have measured the absorption length for 25 GeV and 50 GeV π^-'s incident on this detector. It is 188±7 cm. (The liquid density is 0.86 gm/cm^3.)

3. We use Nuclear Enterprise Corporation liquid scintillator NE235A.

4. American Durafilm, Newton, Mass., supplies teflon film. Hy-Sil, Revere, Mass., evaporates aluminum onto the teflon. Material Distributors Corp., Woburn, Mass., adds the adhesive and mylar backing.

5. See presentation at this conference by R. Imlay, "Tests of a Prototype Lead-Liquid Scintillator Calorimeter Module for FNAL Experiment 310."

6. RTV 733, Dow Corning Corp.

7. Available from Nuclear Enterprises Corporation.

8. Sylgard 188 encapsulating resin, Dow Corning Co.

9. The bulk price per tube is $40.00.

10. See contributions by T. Gabriel to this conference and "Response of a Large All-Liquid Scintillator Spectrometer and of a 24 Layer Iron-Plastic Spectrometer to Charged Pions and Protons in the Low - GeV Energy Range", T. A. Gabriel and J. D. Amburgey, ORNL-TM-4349, Oak Ridge Reprint.

11. From the contribution to this conference, "Design and Performance of a Liquid Scintillator/Iron Sandwich Calorimeter Used at the ISR", L. Baum, H. Hilscher, F. Lobkovicz, C. Rubbia, A. Straude, presented by H. Hilscher.

12. See Appendix 2, "A Detailed Discussion of the Target Calorimeter to Determine both Energy and Duration of the Hadronic Jet" of FNAL Proposal #310, by A. Benvenuti et al.

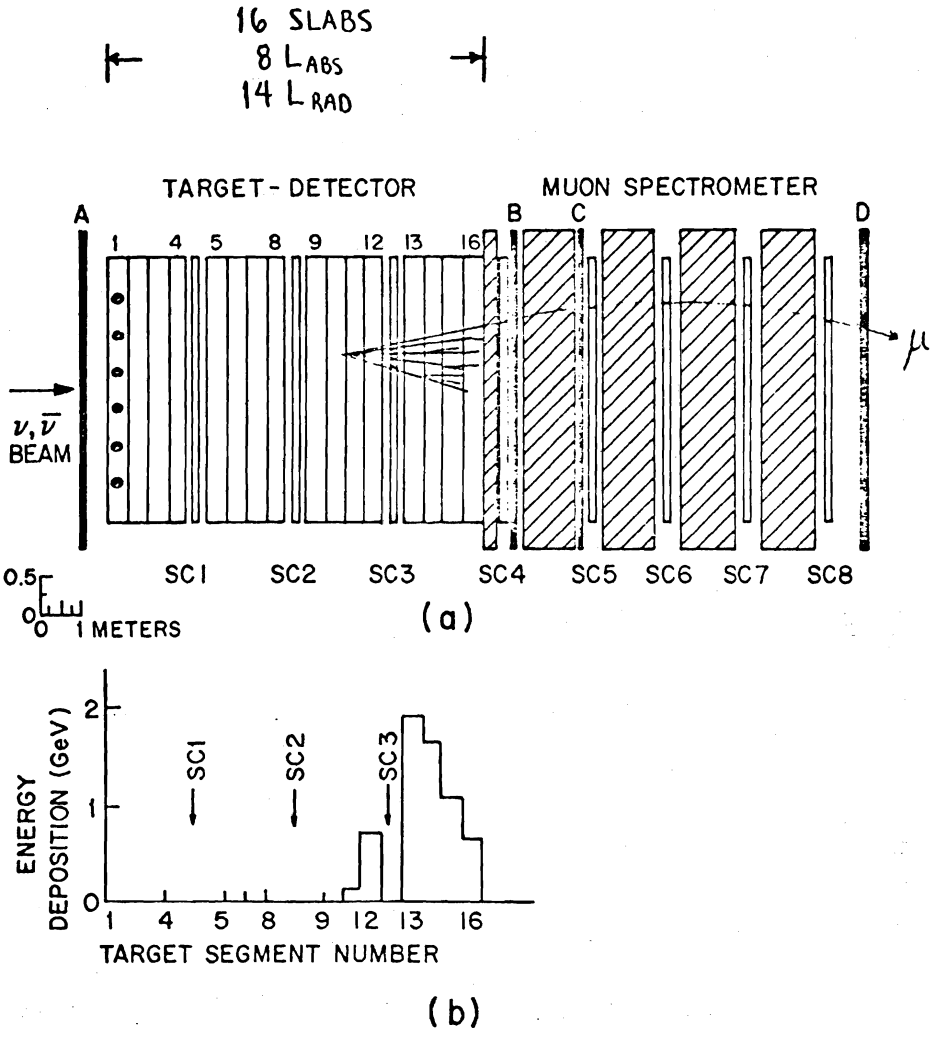
16 SLABS
8 L_{ABS}
14 L_{RAD}
TARGET - DETECTOR
MUON SPECTROMETER
A
B
C
D
1 4 5 8 9 12 13 16
$\nu, \bar{\nu}$ BEAM
μ
0.5
0 1 METERS
SC1 SC2 SC3 SC4 SC5 SC6 SC7 SC8
(a)
ENERGY DEPOSITION (GeV)
2
1
0
SC1
SC2
SC3
1 4 5 8 9 12 13 16
TARGET SEGMENT NUMBER
(b)

Figure 1

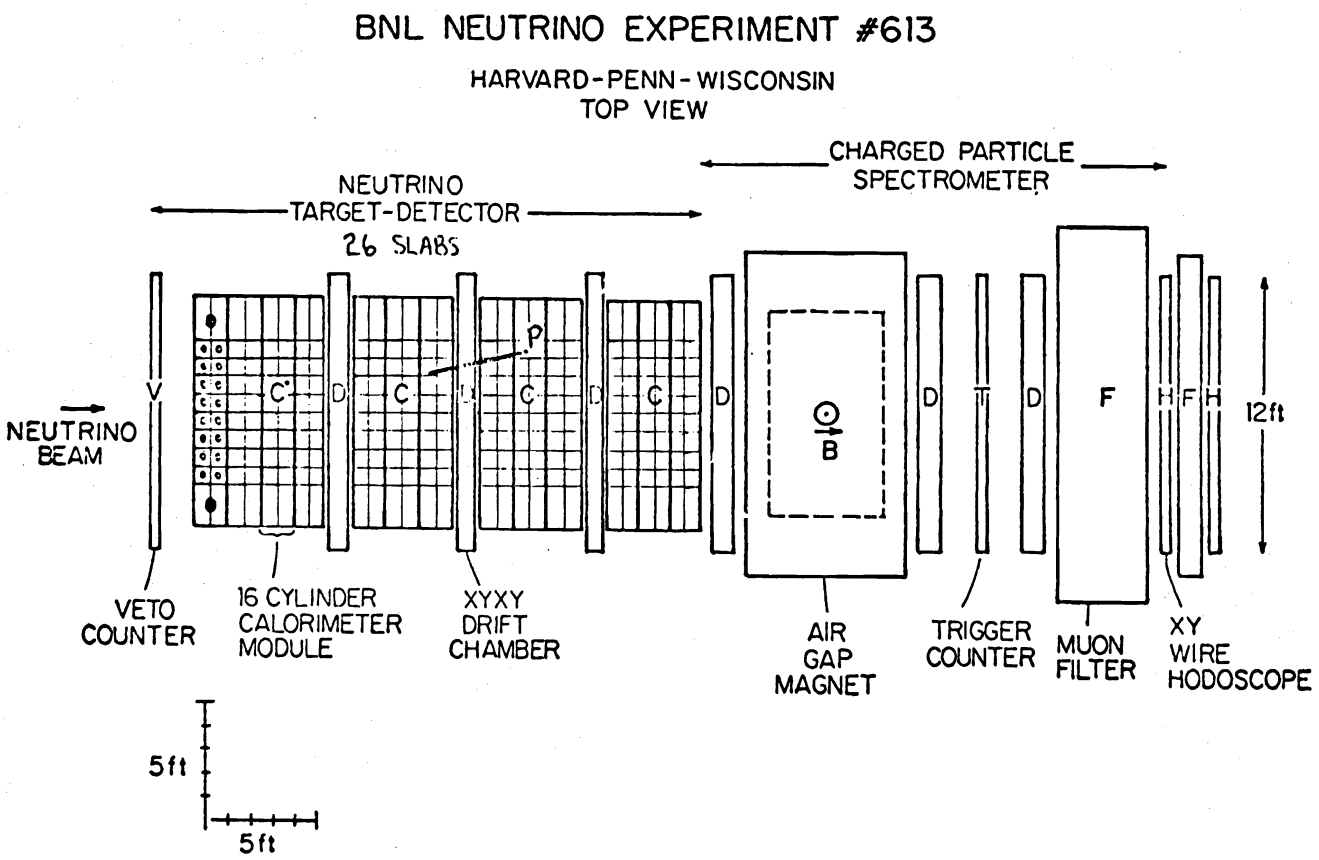
BNL NEUTRINO EXPERIMENT #613
HARVARD-PENN-WISCONSIN
TOP VIEW
CHARGED PARTICLE
SPECTROMETER
NEUTRINO
TARGET-DETECTOR
26 SLABS
NEUTRINO
BEAM
V
C
D
C
P
C
D
C
D
B
D
T
D
F
H
F
H
12ft
VETO
COUNTER
16 CYLINDER
CALORIMETER
MODULE
XYXY
DRIFT
CHAMBER
AIR
GAP
MAGNET
TRIGGER
COUNTER
MUON
FILTER
XY
WIRE
HODOSCOPE
5ft
5ft

Figure 2

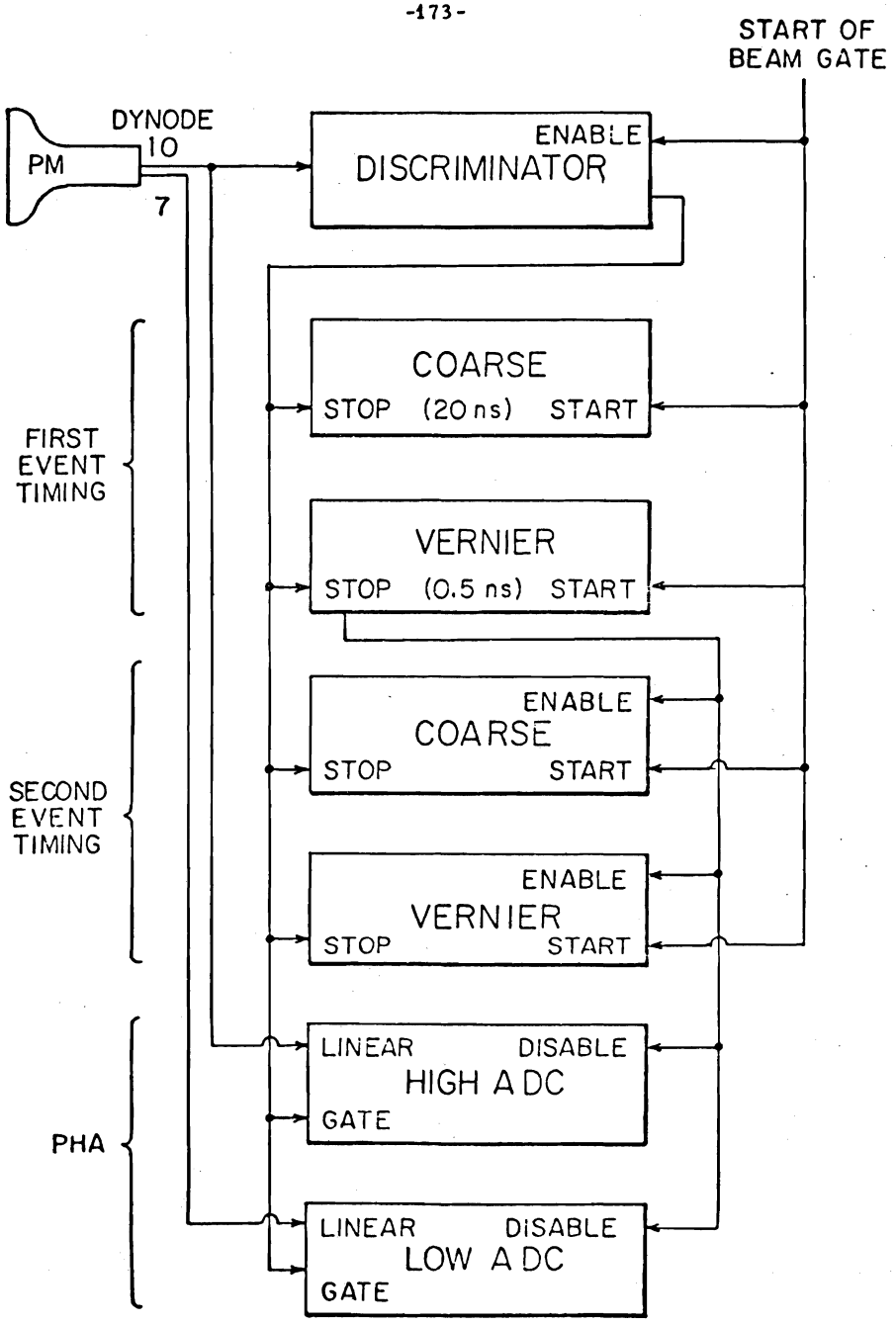
START OF
BEAM GATE
DYNODE
10
PM
7
ENABLE
DISCRIMINATOR
COARSE
STOP (20 ns) START
VERNIER
STOP (0.5 ns) START
ENABLE
COARSE
STOP START
ENABLE
VERNIER
STOP START
LINEAR DISABLE
HIGH A DC
GATE
LINEAR DISABLE
LOW A DC
GATE
FIRST
EVENT
TIMING
SECOND
EVENT
TIMING
PHA

Figure 3

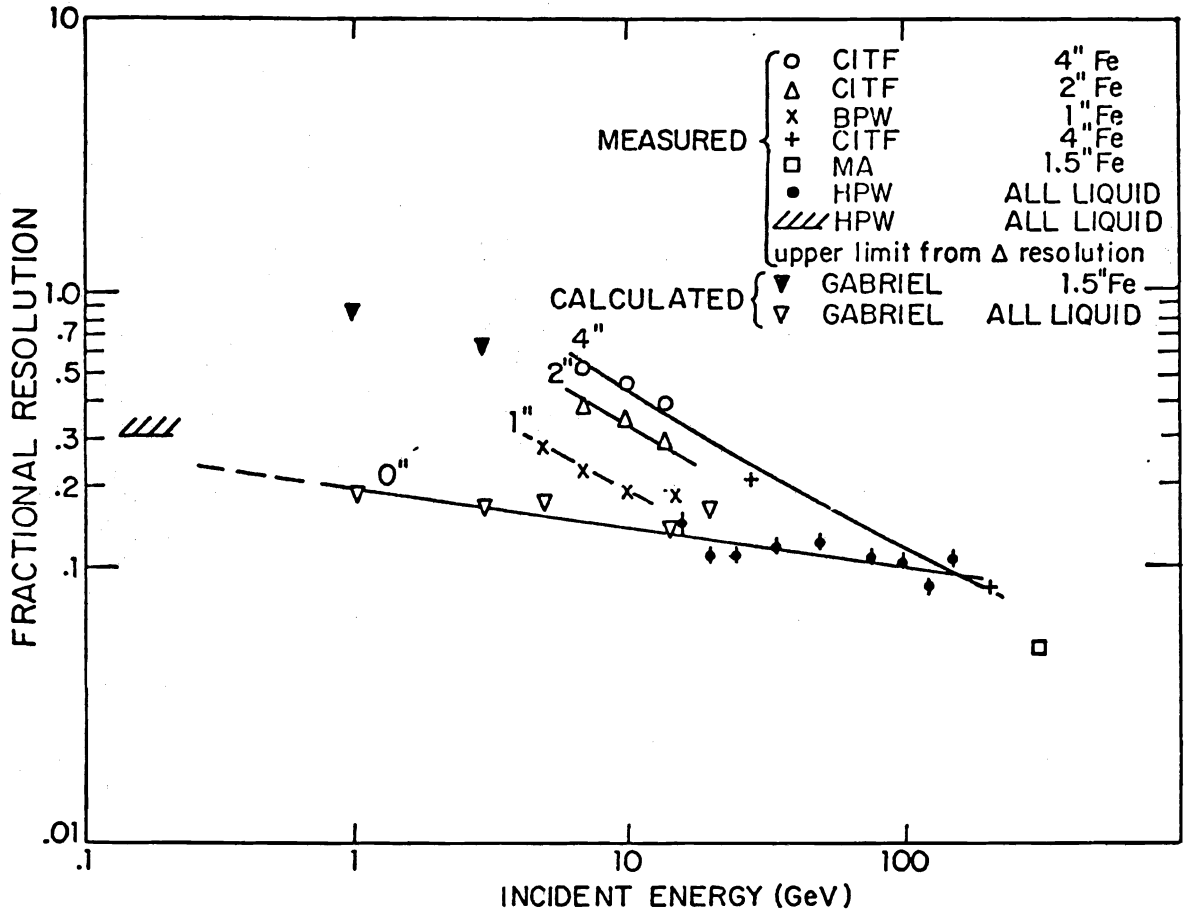
10
1.0
.7
.5
.3
.2
.1
.01
.1
1
10
100
FRACTIONAL RESOLUTION
INCIDENT ENERGY (GeV)
MEASURED
CITF 4" Fe
CITF 2" Fe
BPW 1" Fe
CITF 4" Fe
MA 1.5" Fe
HPW ALL LIQUID
HPW ALL LIQUID
upper limit from Δ resolution
CALCULATED
GABRIEL 1.5"Fe
GABRIEL ALL LIQUID
4"
2"
1"
0"

Figure 4

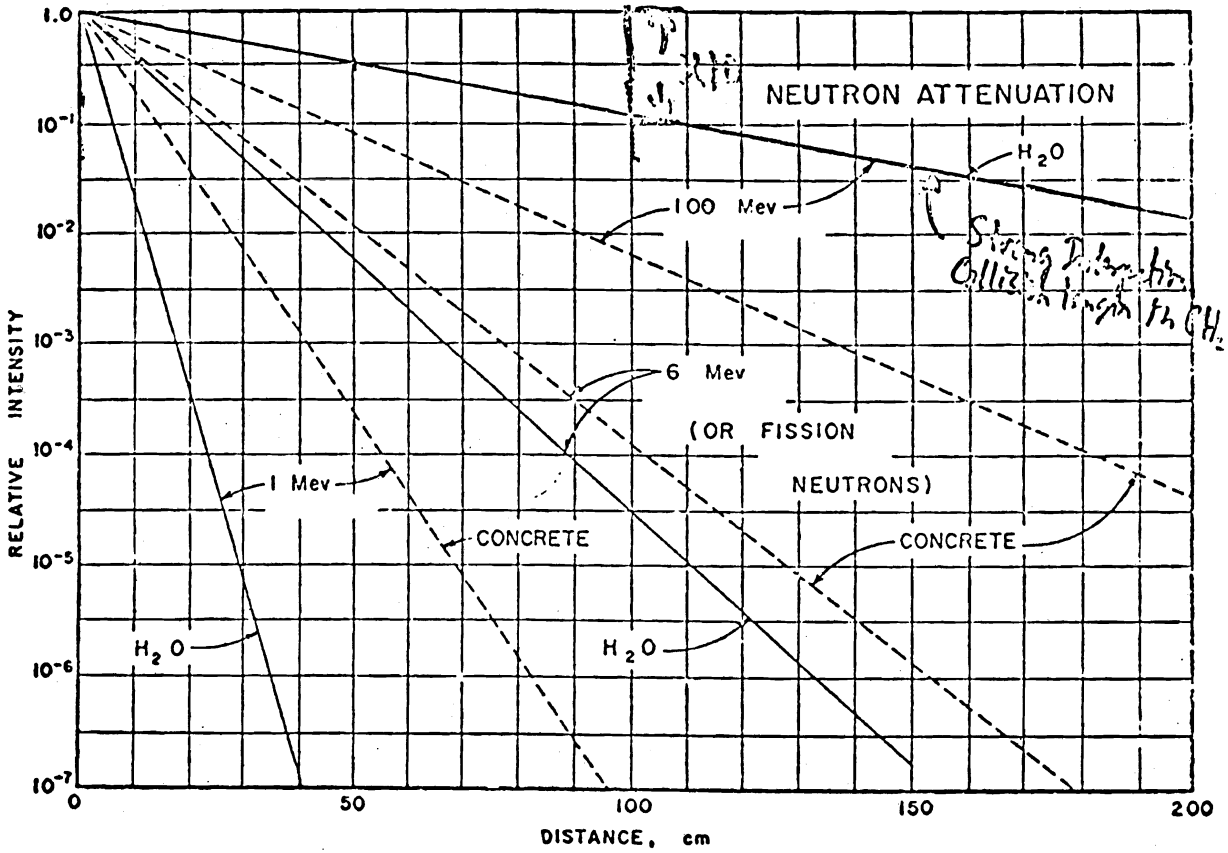
NEUTRON ATTENUATION
RELATIVE INTENSITY
1.0
10^{-1}
10^{-2}
10^{-3}
10^{-4}
10^{-5}
10^{-6}
10^{-7}
0
50
100
150
200
DISTANCE, cm
H_2O
100 Mev
6 Mev
(OR FISSION
NEUTRONS)
1 Mev
CONCRETE
CONCRETE
H_2O
H_2O

Figure 5

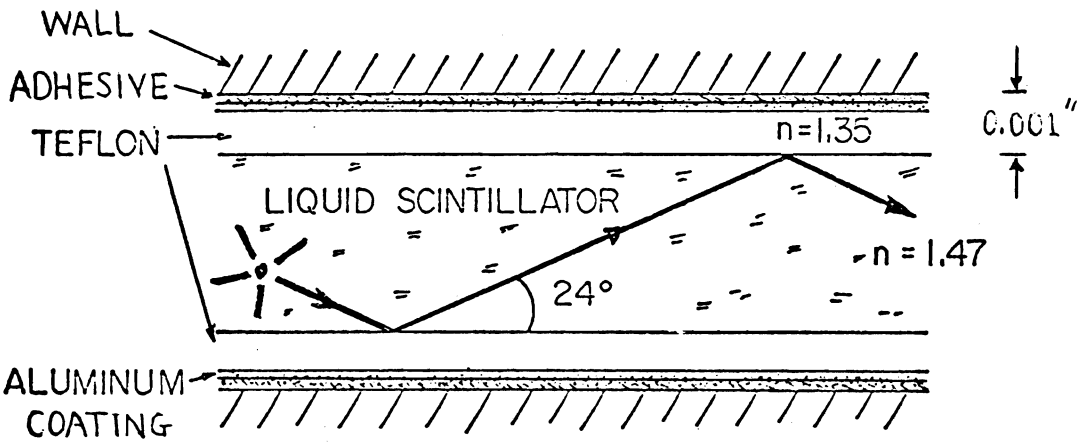
WALL
ADHESIVE
TEFLON
n=1.35
0.001"
LIQUID SCINTILLATOR
n = 1.47
24°
ALUMINUM
COATING

Figure 6

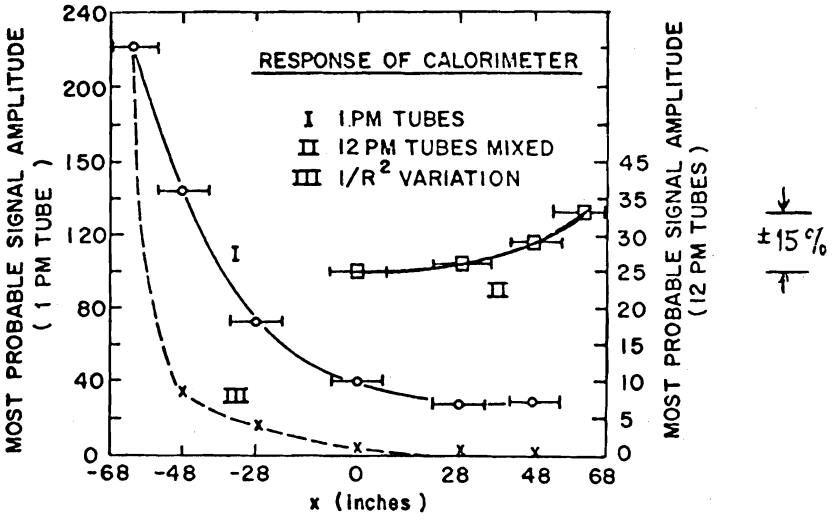
RESPONSE OF CALORIMETER
I 1 PM TUBES
II 12 PM TUBES MIXED
III 1/R² VARIATION
MOST PROBABLE SIGNAL AMPLITUDE (1 PM TUBE)
MOST PROBABLE SIGNAL AMPLITUDE (12 PM TUBES)
x (inches)
±15%

Figure 7

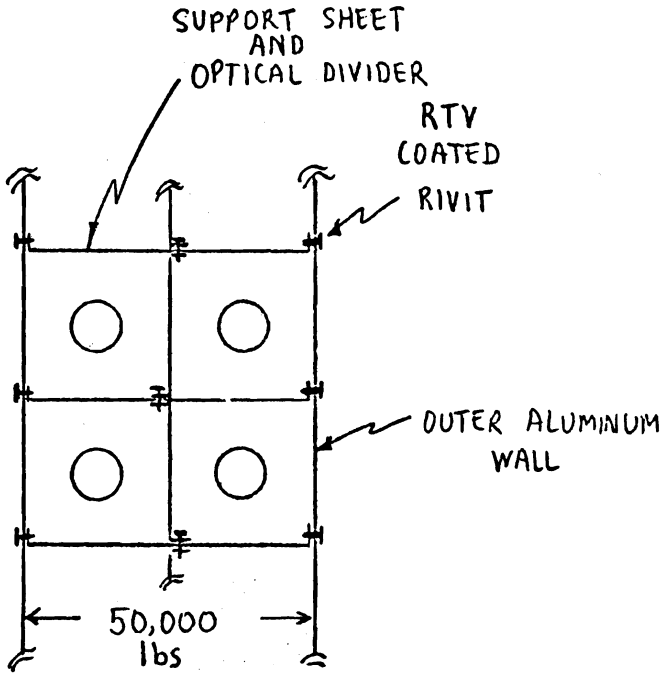
SUPPORT SHEET
AND
OPTICAL DIVIDER
RTV
COATED
RIVIT
OUTER ALUMINUM
WALL
50,000
lbs

Figure 8

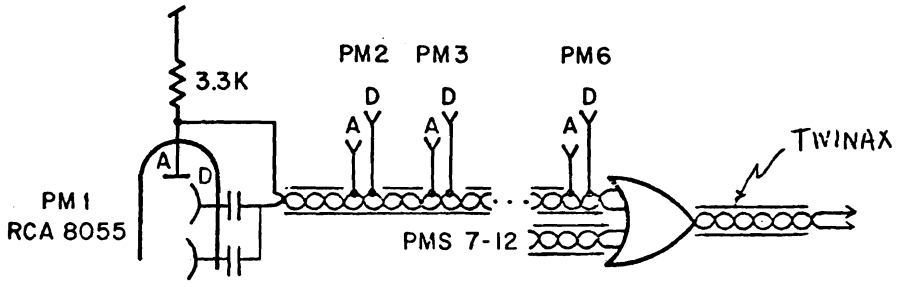

Figure 9

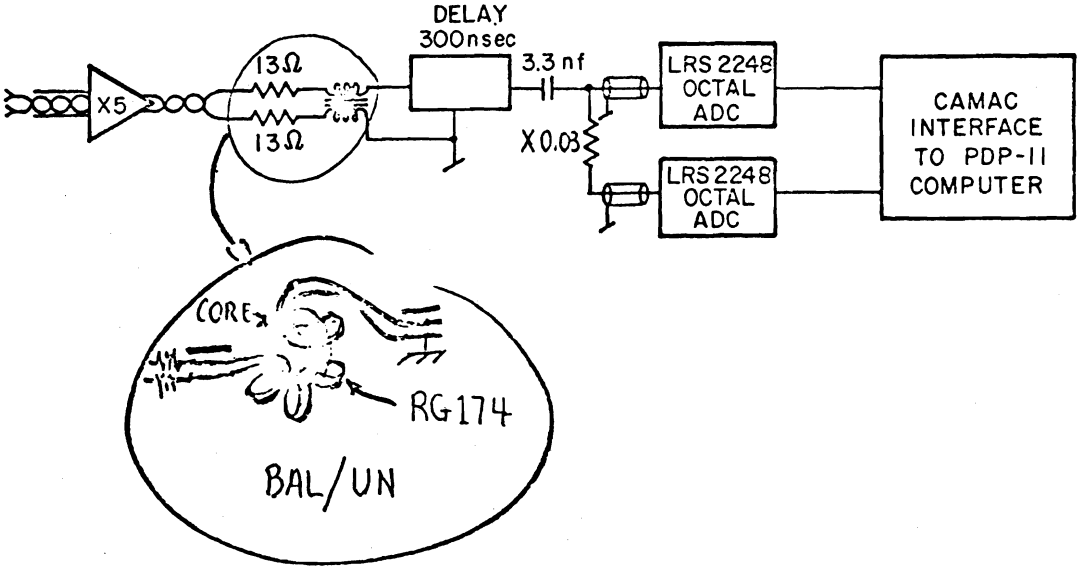

Figure 10

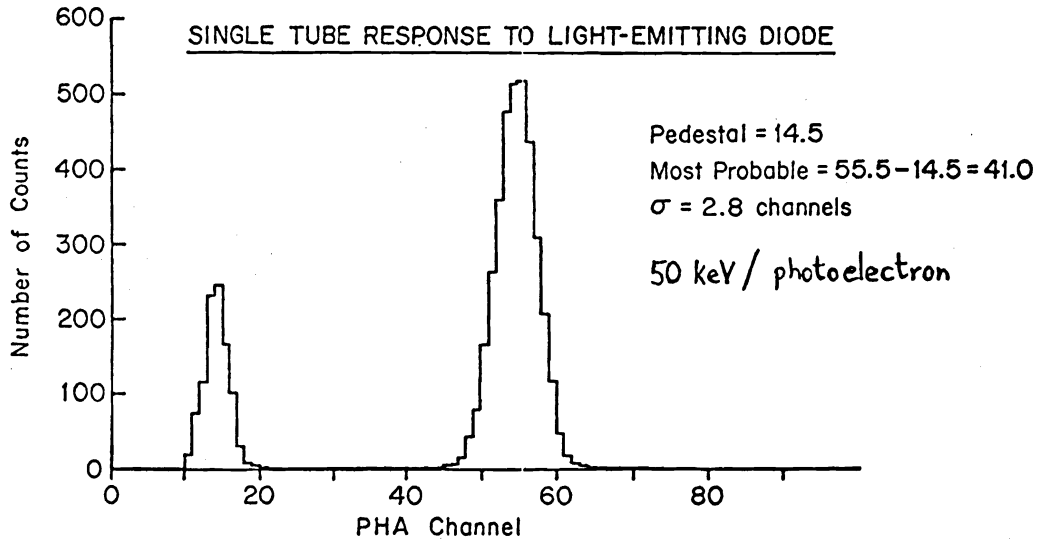
SINGLE TUBE RESPONSE TO LIGHT-EMITTING DIODE
Number of Counts
600
500
400
300
200
100
0
0
20
40
60
80
PHA Channel
Pedestal = 14.5
Most Probable = 55.5 − 14.5 = 41.0
σ = 2.8 channels
50 keV / photoelectron

Figure 11

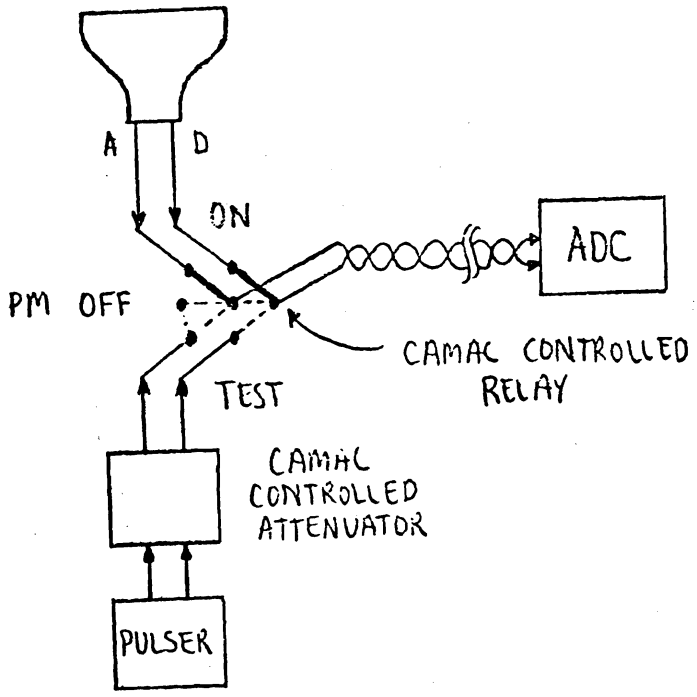
A
D
ON
ADC
PM OFF
CAMAC CONTROLLED
RELAY
TEST
CAMAC
CONTROLLED
ATTENUATOR
PULSER

Figure 12

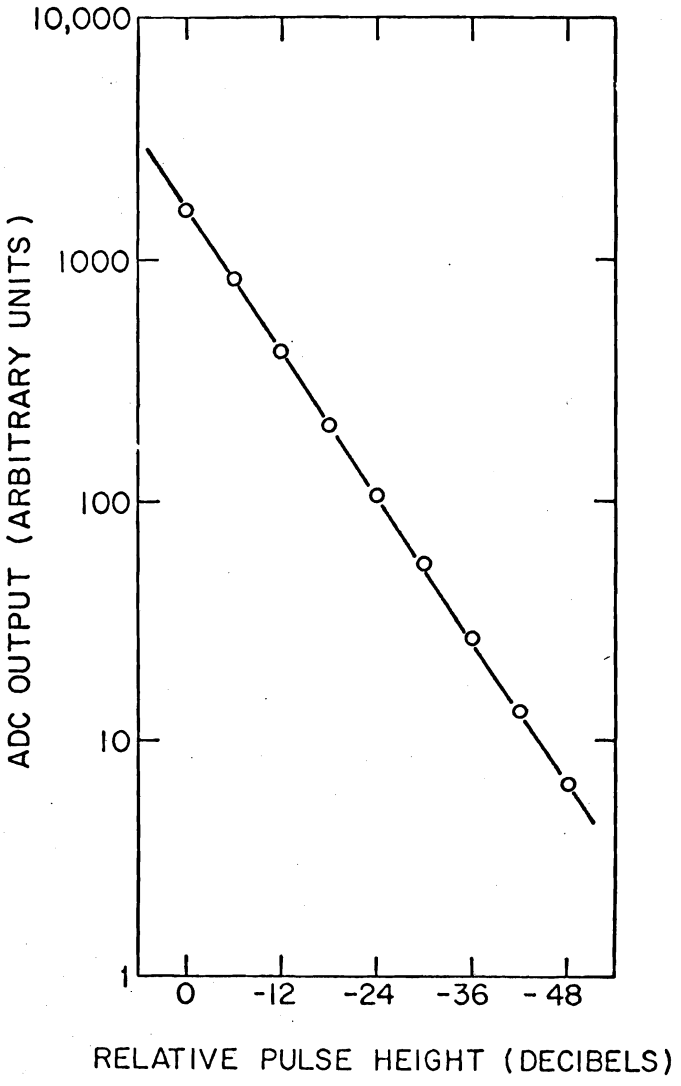
10,000
1000
100
10
1
ADC OUTPUT (ARBITRARY UNITS)
0
-12
-24
-36
-48
RELATIVE PULSE HEIGHT (DECIBELS)

Fig. 13

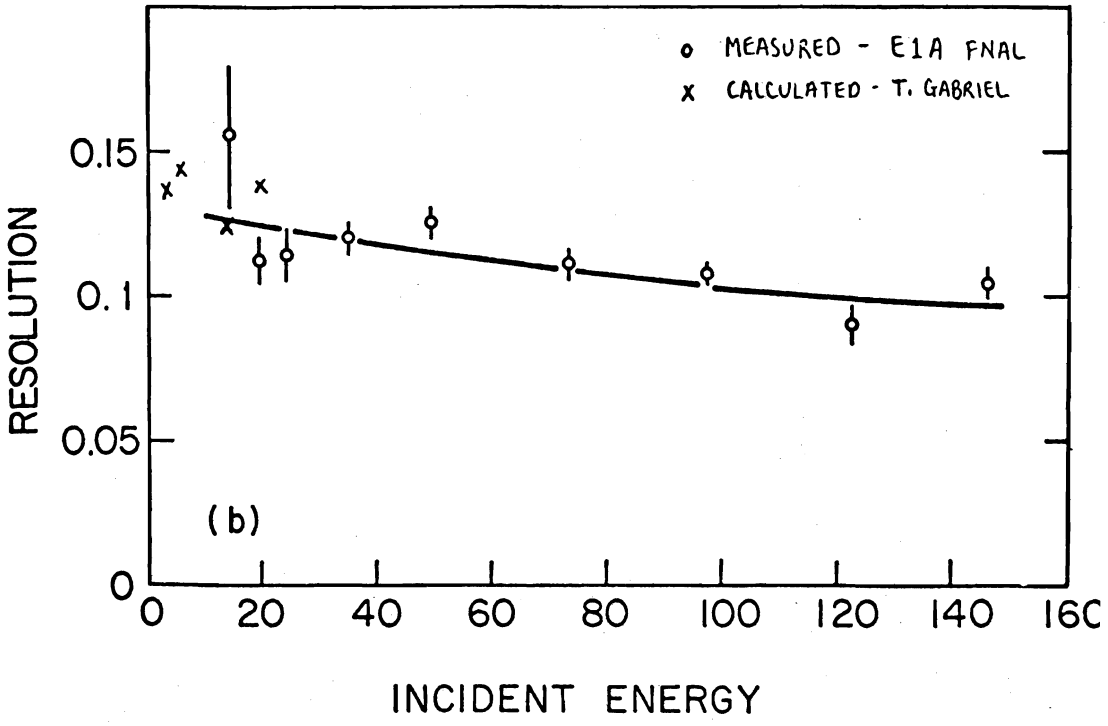
o MEASURED - E1A FNAL
x CALCULATED - T. GABRIEL
RESOLUTION
0.15
0.1
0.05
0
(b)
0
20
40
60
80
100
120
140
160
INCIDENT ENERGY

Figure 14

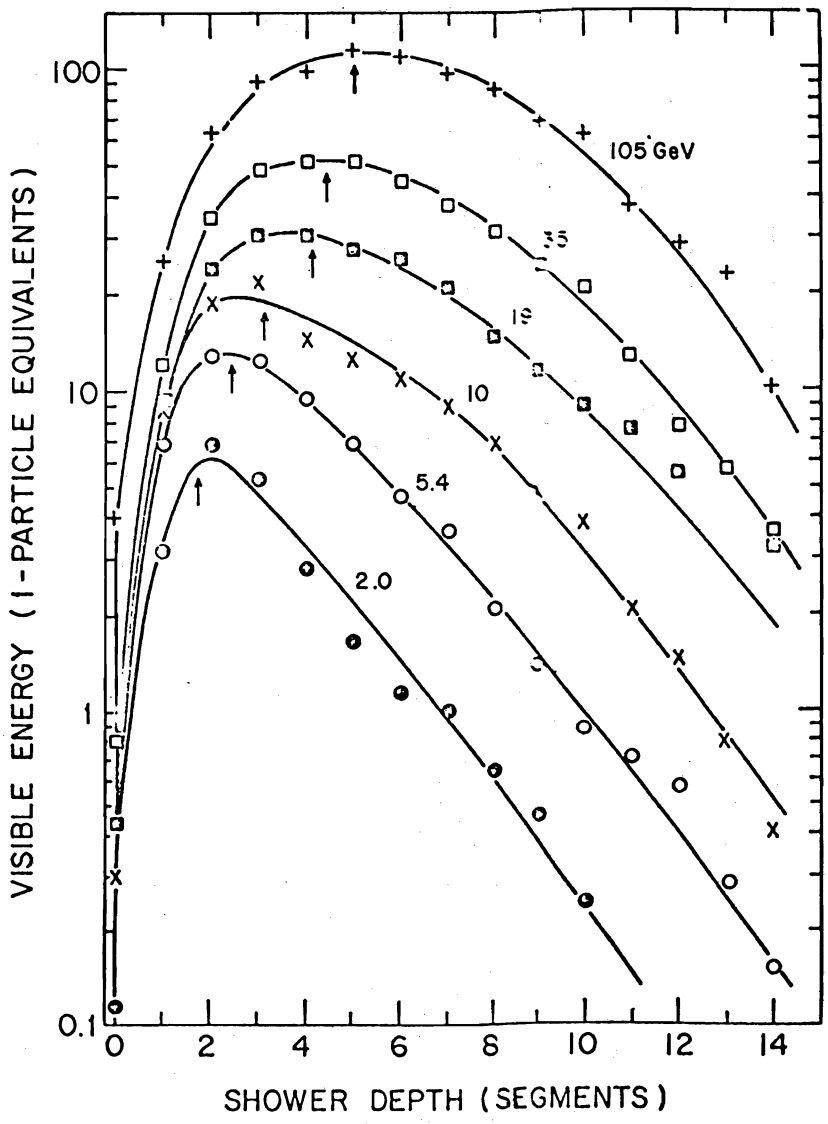
VISIBLE ENERGY (1-PARTICLE EQUIVALENTS)
SHOWER DEPTH (SEGMENTS)
100
10
1
0.1
0
2
4
6
8
10
12
14
105 GeV
10
5.4
2.0

Fig. 15

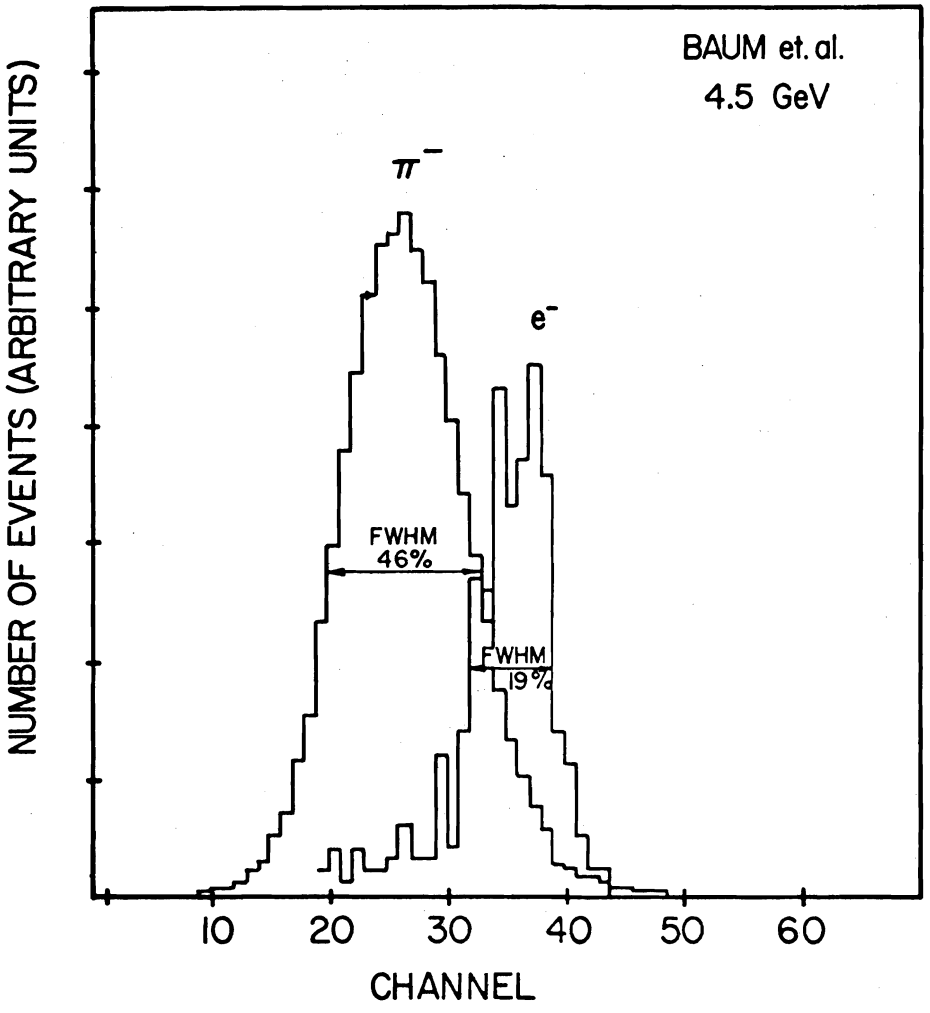
BAUM et. al.
4.5 GeV
π^-
e^-
FWHM
46%
FWHM
19%
NUMBER OF EVENTS (ARBITRARY UNITS)
10
20
30
40
50
60
CHANNEL

FIG. 16

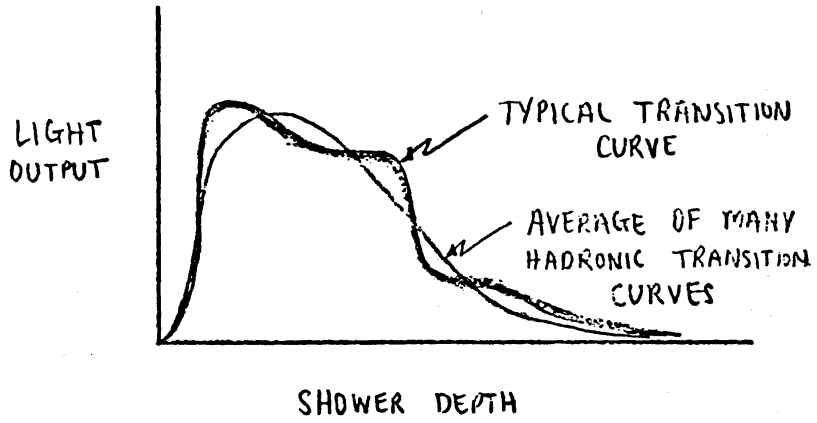
LIGHT
OUTPUT
TYPICAL TRANSITION
CURVE
AVERAGE OF MANY
HADRONIC TRANSITION
CURVES
SHOWER DEPTH

Figure 17

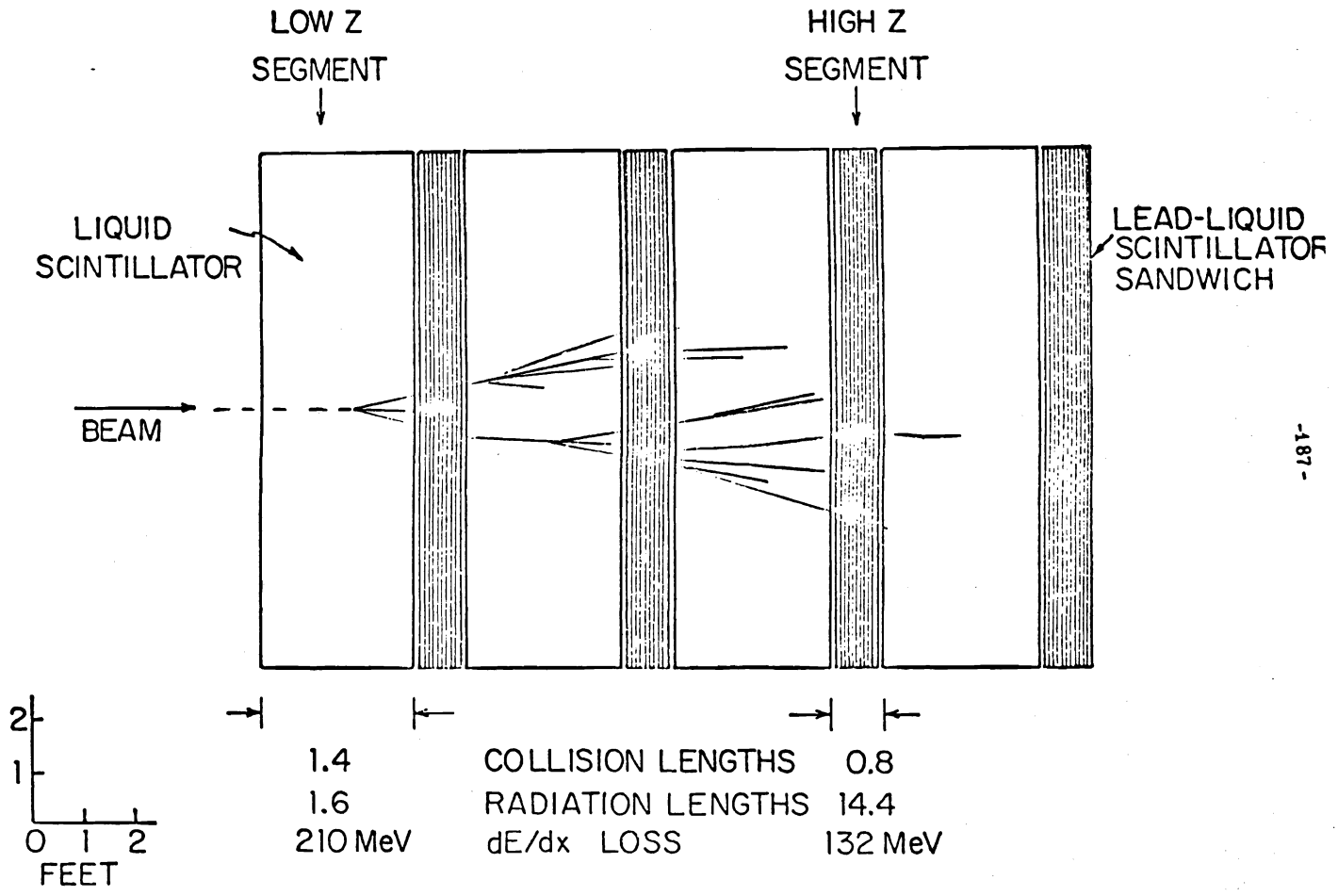
LOW Z
SEGMENT
HIGH Z
SEGMENT
LIQUID
SCINTILLATOR
LEAD-LIQUID
SCINTILLATOR
SANDWICH
BEAM
2
1
0 1 2
FEET
1.4
1.6
210 MeV
COLLISION LENGTHS
RADIATION LENGTHS
dE/dx LOSS
0.8
14.4
132 MeV

Figure 18

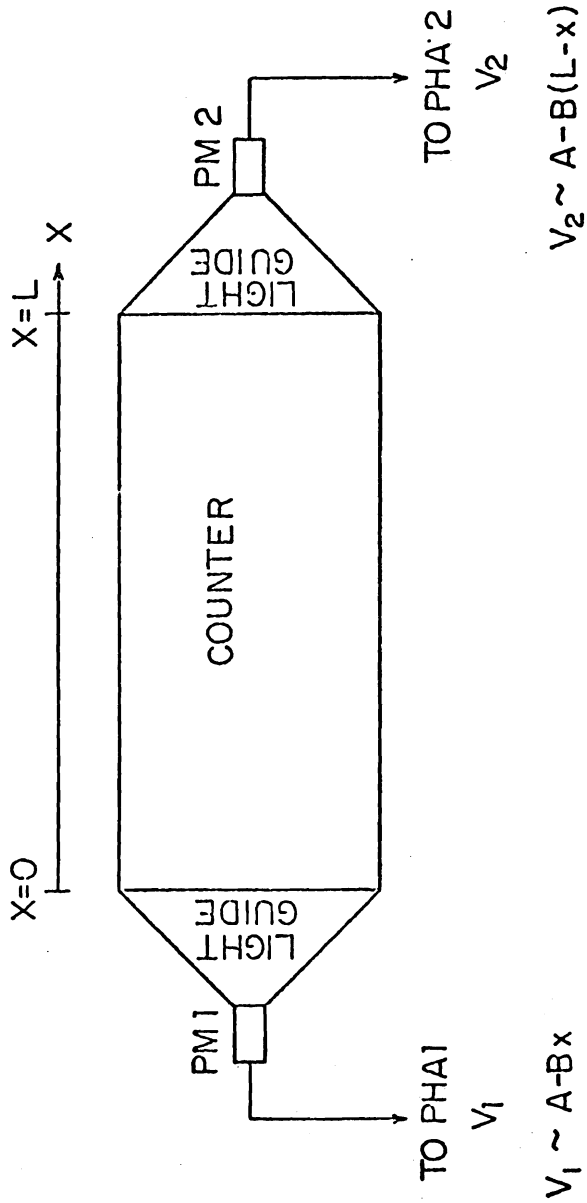
X
X=L
X=O
LIGHT GUIDE
COUNTER
LIGHT GUIDE
PM 2
PM 1
TO PHA 2
TO PHA 1
V_2
V_1
$V_2 \sim A-B(L-x)$
$V_1 \sim A-Bx$

Figure 19

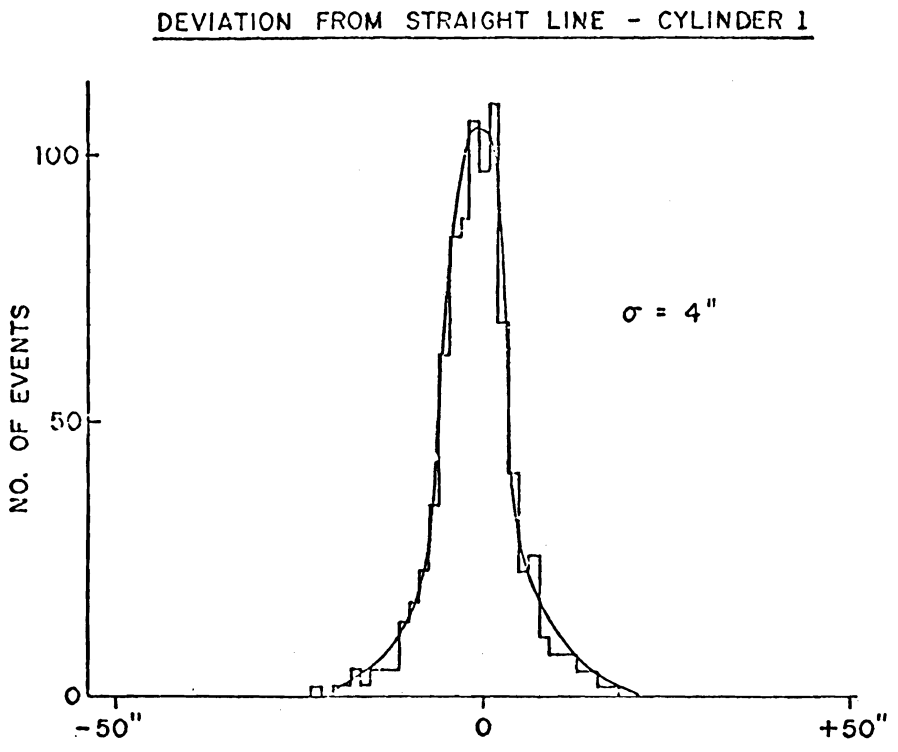
DEVIATION FROM STRAIGHT LINE - CYLINDER 1
NO. OF EVENTS
100
50
0
σ = 4"
-50"
0
+50"

Figure 20